IMU Data Analysis

Adithya Rajendran

1 Introduction

The purpose of this report is to analyze the data collected from an Inertial Measurement Unit (IMU) during two separate stationary tests: a 15-minute test and a 5-hour test. The IMU sensors analyzed include the accelerometer, gyroscope, and magnetometer. The goal is to evaluate sensor noise characteristics and performance through various analyses.

For the 15-minute test, time-series data and histograms for each sensor axis are generated and examined to understand the distribution of the sensor readings during a short stationary period. The histograms are used to observe the normality and spread of the sensor noise.

For the 5-hour test, Allan Variance analysis is conducted to investigate the long-term behavior of the sensor noise. Allan Variance provides insights into different types of noise processes, such as angle random walk, rate random walk, and bias instability, which are essential for understanding IMU performance over extended time intervals.The analyses presented in this report are aimed at quantifying the short-term noise properties and long-term drift behavior of the IMU, which are critical for applications in navigation, robotics, and motion tracking.

2 15-Minute Data Analysis

The 15-minute stationary test data is used to evaluate the short-term performance of the IMU sensors, including the accelerometer, gyroscope, and magnetometer. During this test, the IMU remained stationary, allowing us to analyze the inherent noise and sensor behavior without the influence of external movement.

For each sensor, time-series plots and histograms are generated to visualize and statistically describe the sensor outputs over the stationary period. The time-series plots show the raw data over time, while the histograms give insight into the distribution, mean, and standard deviation of the noise for each axis. These analyses help to assess the short-term precision and stability of the sensors, and to check for normality in the noise distribution, which is important for IMU calibration and error modeling.

2.1 Accelerometer Data Analysis (15-minute dataset)

The accelerometer data captures the linear acceleration experienced by the IMU sensor in the x, y, and z directions. The 15-minute stationary data for the accelerometer is shown in time-series plots and histograms for each axis.

2.1.1 Time-Series Analysis

The time-series plot (Figure 1) demonstrates the accelerations measured over the 15-minute period for the three axes. As expected, the z-axis records the most significant value, around -9.8 m/s^2, which corresponds to the acceleration due to gravity acting downward while the sensor is stationary. The x and y axes, on the other hand, show much smaller accelerations close to zero, indicating minimal movement along these axes.

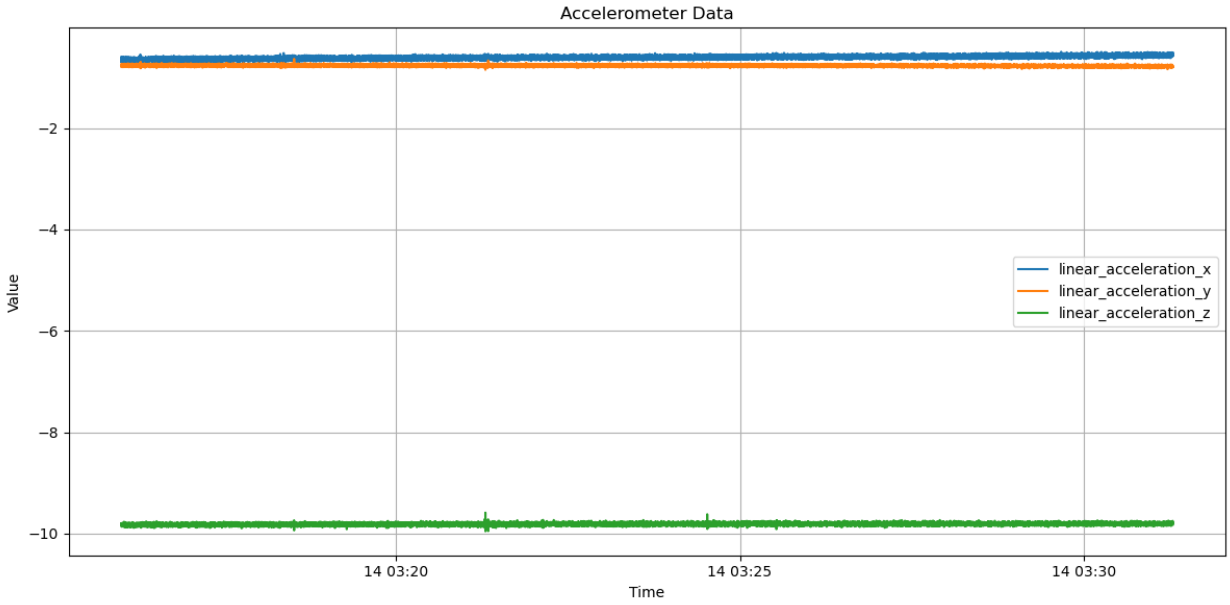

Figure 1: Accelerometer time-series data for 15-minute dataset.

2.1.2 Histogram Analysis

The histograms provide further insight into the distribution of the accelerometer data:

- **X-axis:** The histogram for the x-axis (Figure 2) shows a nearly symmetric Gaussian distribution centered around $\mu = -0.601583$ with a standard deviation of $\sigma = 0.033823$. The slight offset from zero suggests a minor bias or tilt in the sensor's x-axis.
- **Y-axis:** The y-axis histogram (Figure 3) also displays a Gaussian distribution centered around $\mu = -0.764820$ with a smaller standard deviation of $\sigma = 0.015197$. The values indicate a consistent small negative acceleration on this axis, which could again be due to slight tilt or sensor bias.
- **Z-axis:** The z-axis histogram (Figure 4) is centered around $\mu = -9.813524$ with a standard deviation of $\sigma = 0.020554$. This is close to the expected gravitational acceleration, indicating the sensor is accurately capturing the force of gravity when stationary. The small spread suggests low noise in this axis, which is consistent with the stationary condition.

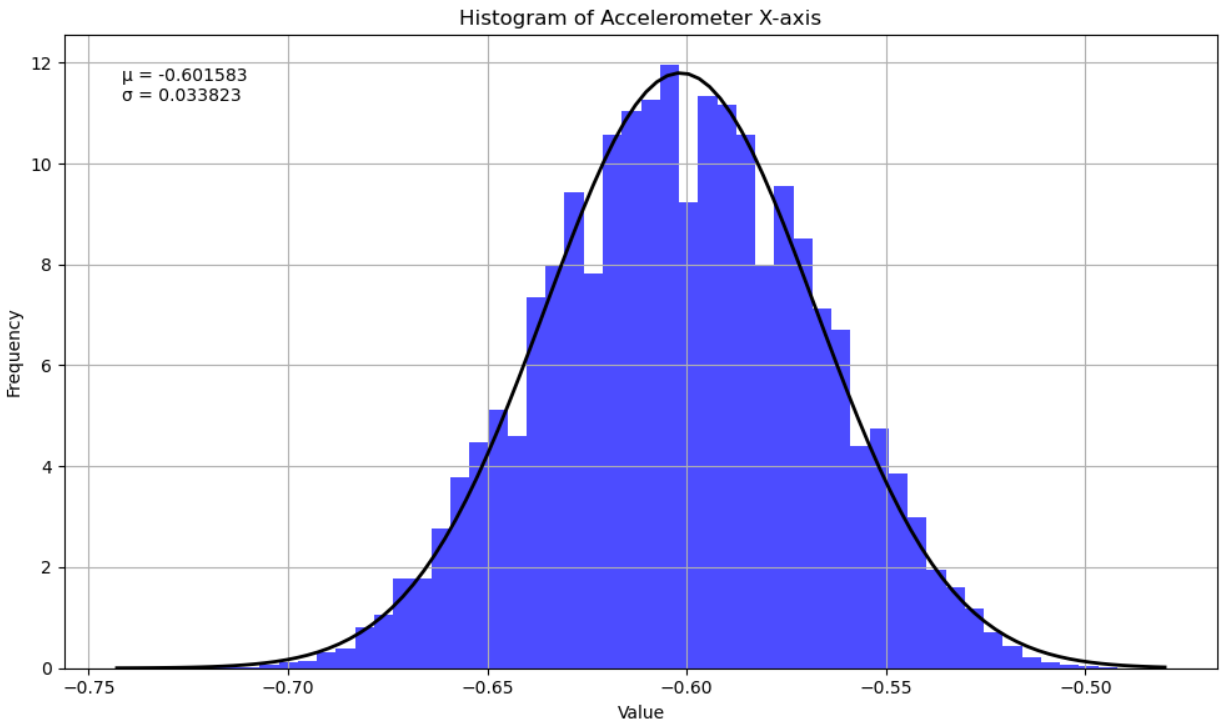

Figure 2: Histogram of accelerometer x-axis for 15-minute dataset.

These analyses show that the accelerometer data conforms well to expectations for a stationary IMU, with Gaussian noise distribution and minor offsets likely due to sensor calibration errors.

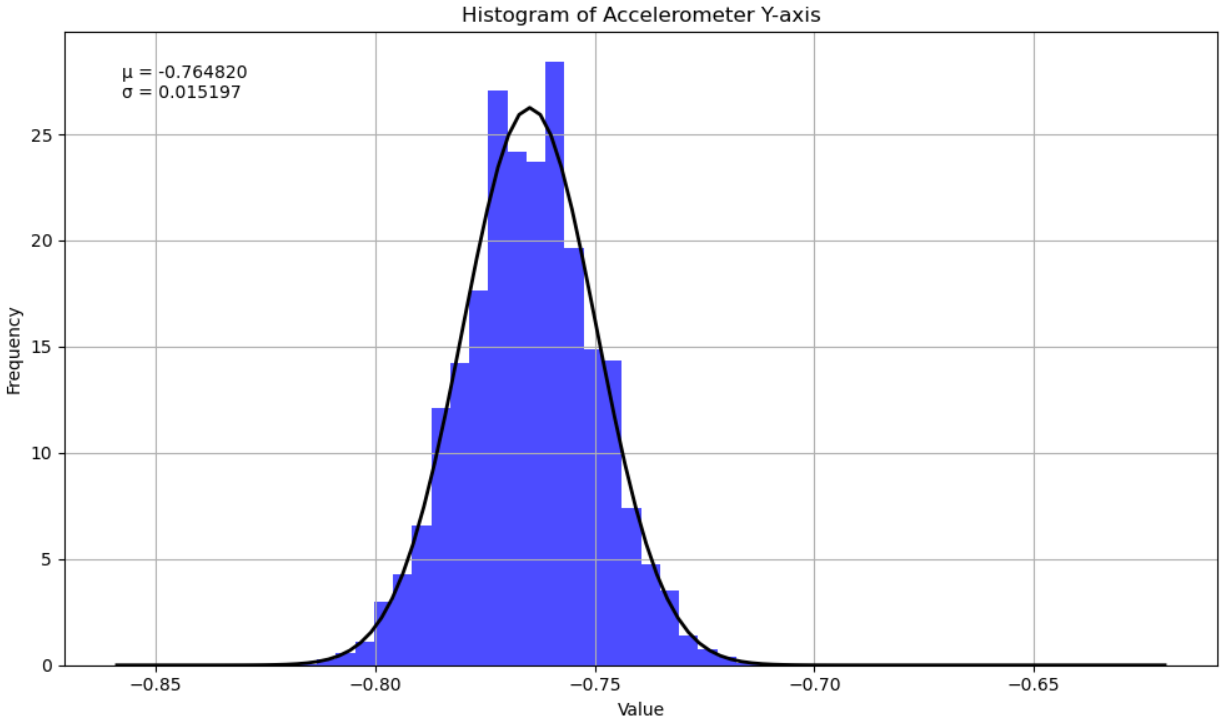

Figure 3: Histogram of accelerometer y-axis for 15-minute dataset.

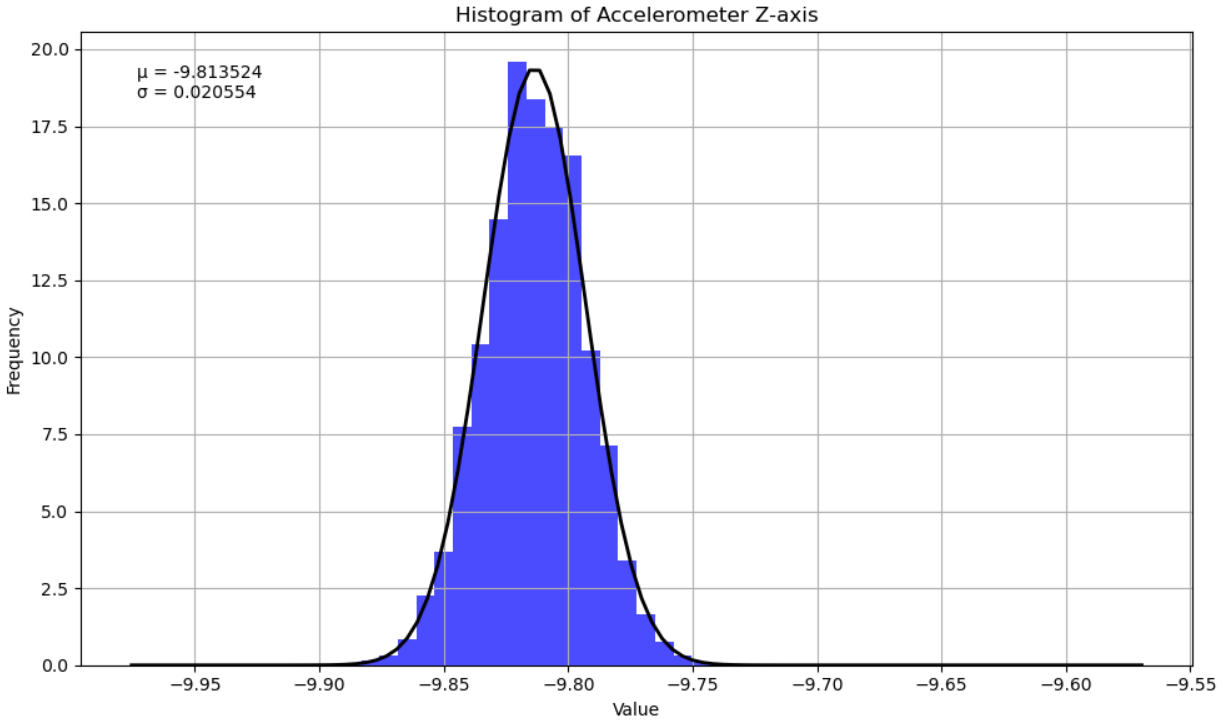

Figure 4: Histogram of accelerometer z-axis for 15-minute dataset.

2.2 Gyroscope Data Analysis (15-minute dataset)

The gyroscope measures the angular velocity of the IMU in the x, y, and z axes. The 15-minute stationary data for the gyroscope is presented below with time-series plots and histograms for each axis.

2.2.1 Time-Series Analysis

The time-series plot (Figure 5) illustrates the angular velocities recorded by the gyroscope over the 15-minute period. The gyroscope data is centered around zero for all three axes, indicating minimal rotational movement during the stationary condition. Some small fluctuations are observed, which likely represent sensor noise.

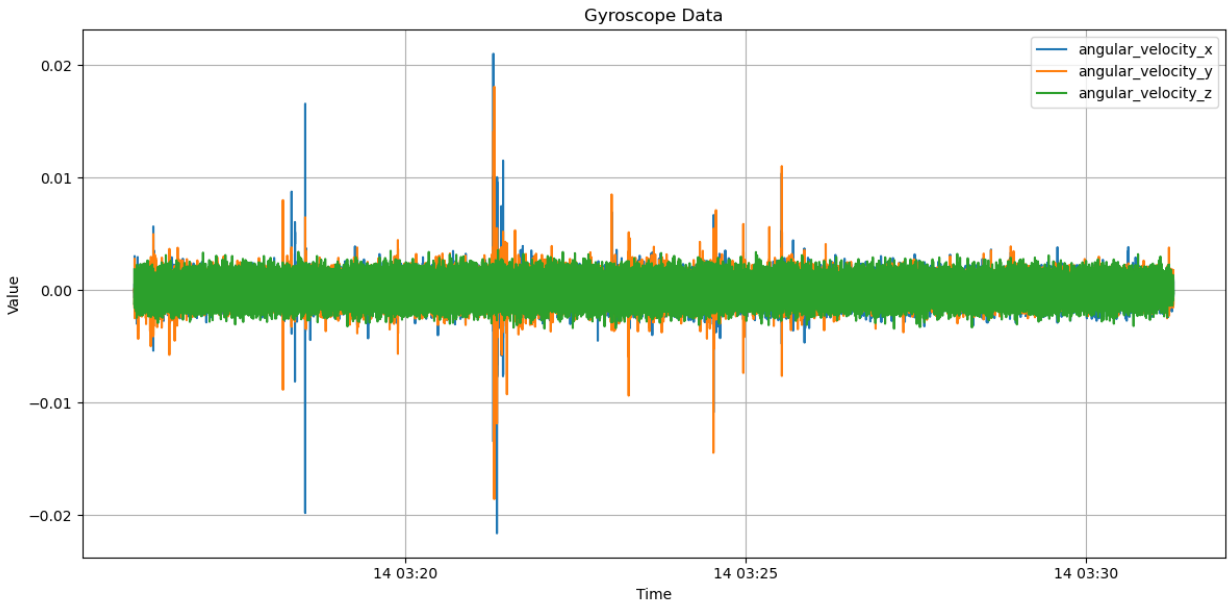

Figure 5: Gyroscope time-series data for 15-minute dataset.

2.2.2 Histogram Analysis

The histograms provide a more detailed view of the distribution of the angular velocities:

- **X-axis:** The histogram for the x-axis (Figure 6) shows a Gaussian distribution centered around $\mu = -0.000022$ with a standard deviation of $\sigma = 0.000954$. This indicates very low angular velocity, with noise centered around zero, as expected for stationary data.
- **Y-axis:** The y-axis histogram (Figure 7) similarly has a Gaussian distribution with $\mu = 0.000030$ and a standard deviation of $\sigma = 0.000945$. Again, the values are close to zero, suggesting minimal rotational movement along this axis.
- **Z-axis:** The z-axis histogram (Figure 8) is centered around $\mu = -0.000003$ with a standard deviation of $\sigma = 0.001067$. The spread is slightly larger than that of the x and y axes, possibly due to a small amount of residual rotational noise in the z-axis.

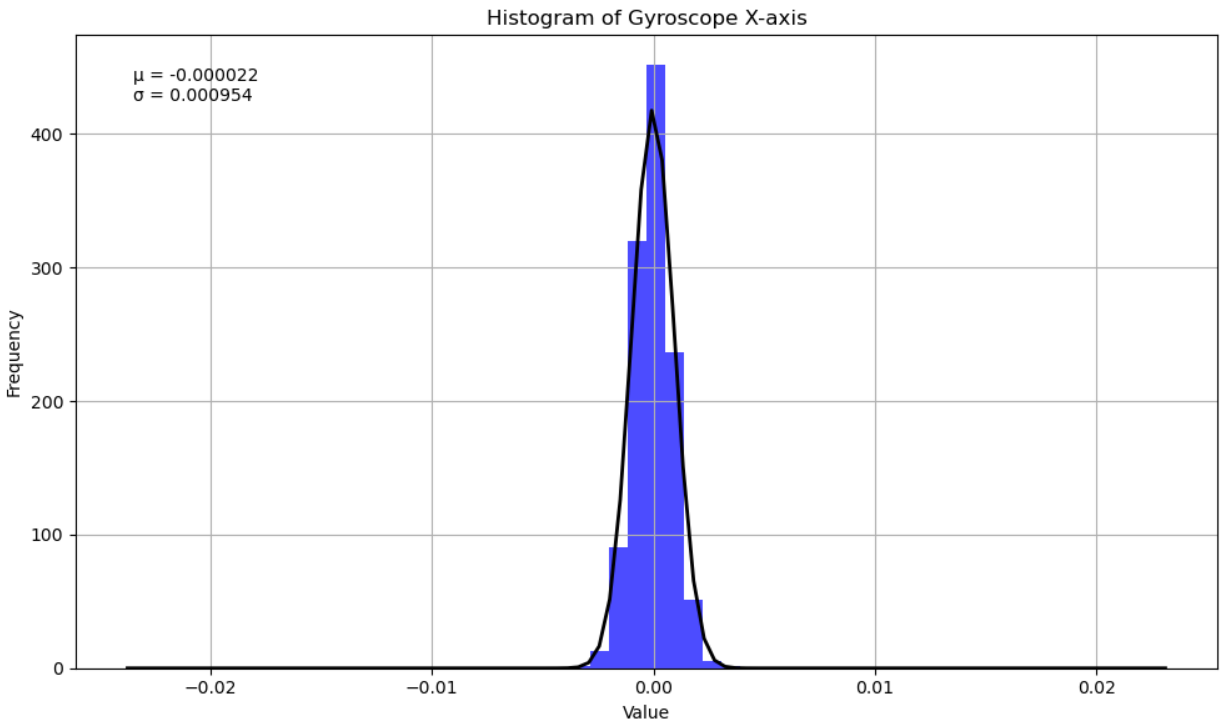

Figure 6: Histogram of gyroscope x-axis for 15-minute dataset.

The gyroscope data shows a small amount of noise in all axes, but the distributions are centered around zero, confirming that the sensor was not experiencing significant rotational movement during the stationary period.

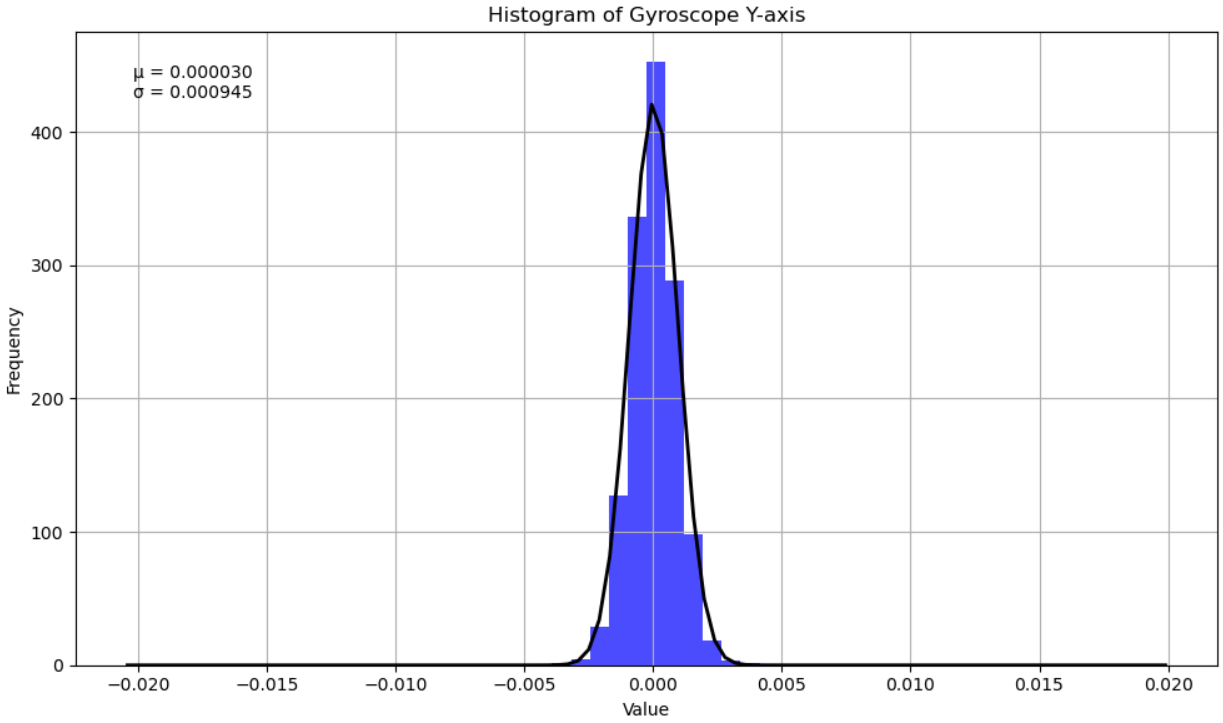

Figure 7: Histogram of gyroscope y-axis for 15-minute dataset.

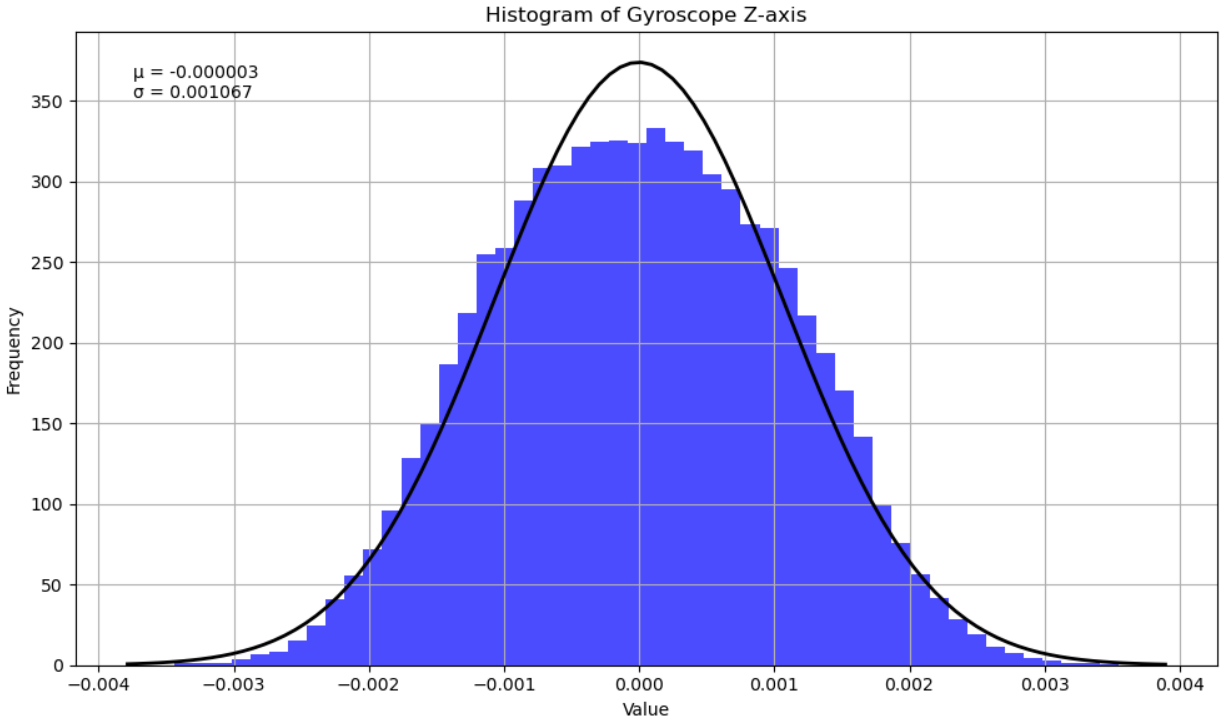

Figure 8: Histogram of gyroscope z-axis for 15-minute dataset.

2.3 Magnetometer Data Analysis (15-minute dataset)

The magnetometer measures the magnetic field strength in the x, y, and z axes. The following sections provide a detailed time-series and histogram analysis of the 15-minute stationary magnetometer data.

2.3.1 Time-Series Analysis

The time-series plot (Figure 9) shows the variations in magnetic field strength for the x, y, and z axes over the 15-minute period. The values remain relatively constant, reflecting the stationary nature of the sensor during the measurement period. Small variations could be attributed to noise or environmental interference.

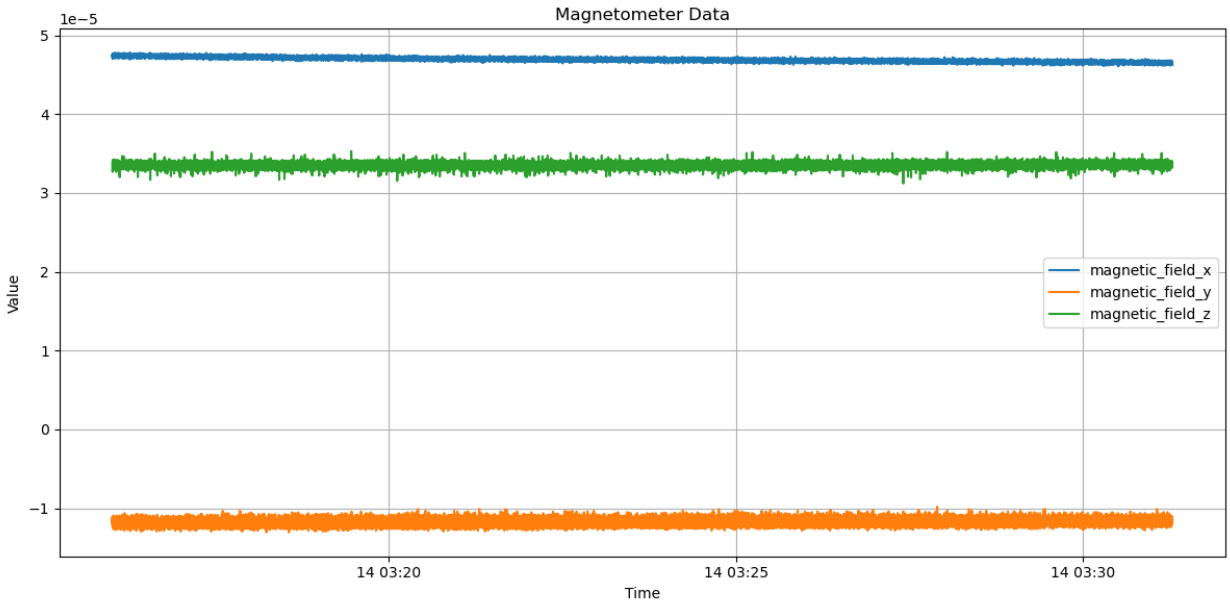

Figure 9: Magnetometer time-series data for 15-minute dataset.

2.3.2 Histogram Analysis

The histograms provide insight into the distribution of magnetic field measurements along each axis:

- **X-axis:** The x-axis histogram (Figure 10) shows a Gaussian distribution centered around $\mu = 4.7 \times 10^{-5}$ with a standard deviation of $\sigma = 0.0$. This indicates that the magnetic field strength in this axis remained almost constant, with minimal noise.
- **Y-axis:** The y-axis histogram (Figure 11) is centered around $\mu = -1.2 \times 10^{-5}$ with a standard deviation of $\sigma = 0.0$. The narrow distribution suggests that the magnetic field strength along this axis also remained steady, with minimal noise during the stationary period.

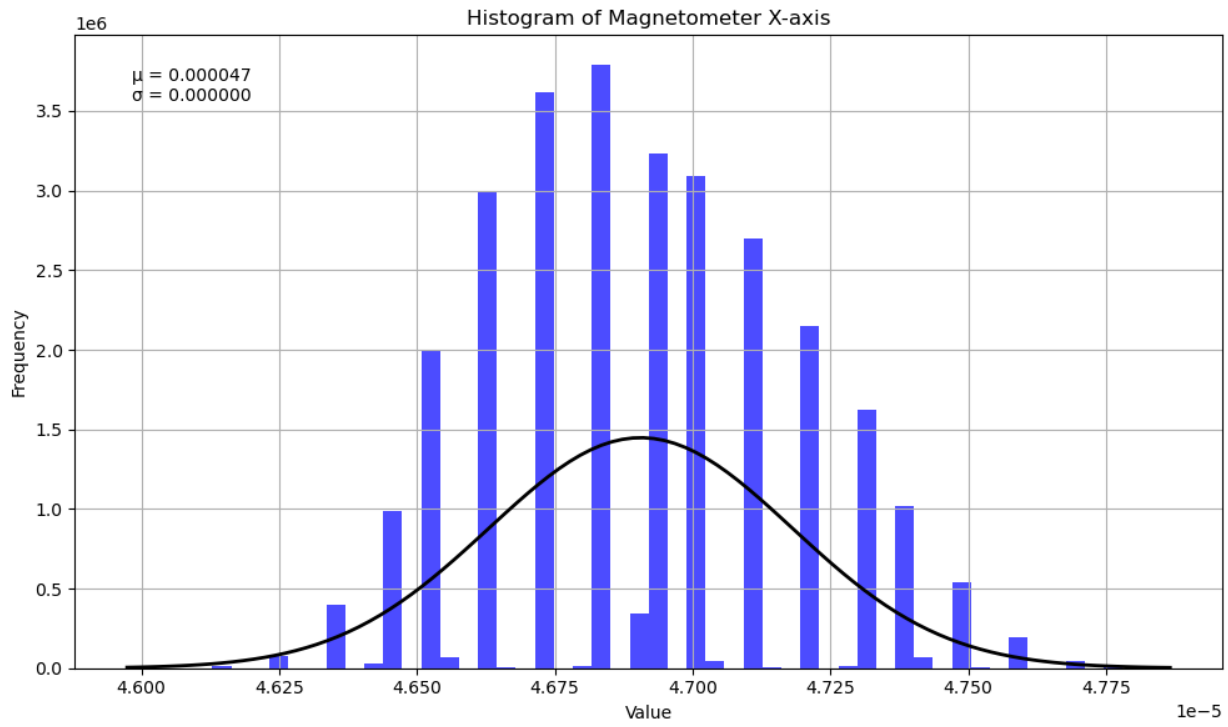

Figure 10: Histogram of magnetometer x-axis for 15-minute dataset.

- **Z-axis:** The z-axis histogram (Figure 12) is centered around $\mu = 3.4 \times 10^{-5}$ with a standard deviation of $\sigma = 0.0$. This distribution reflects minimal variations in the magnetic field strength along the z-axis.

The magnetometer data shows stable measurements for all three axes, with very little noise. This is expected given the stationary conditions of the IMU during the 15-minute data collection period.

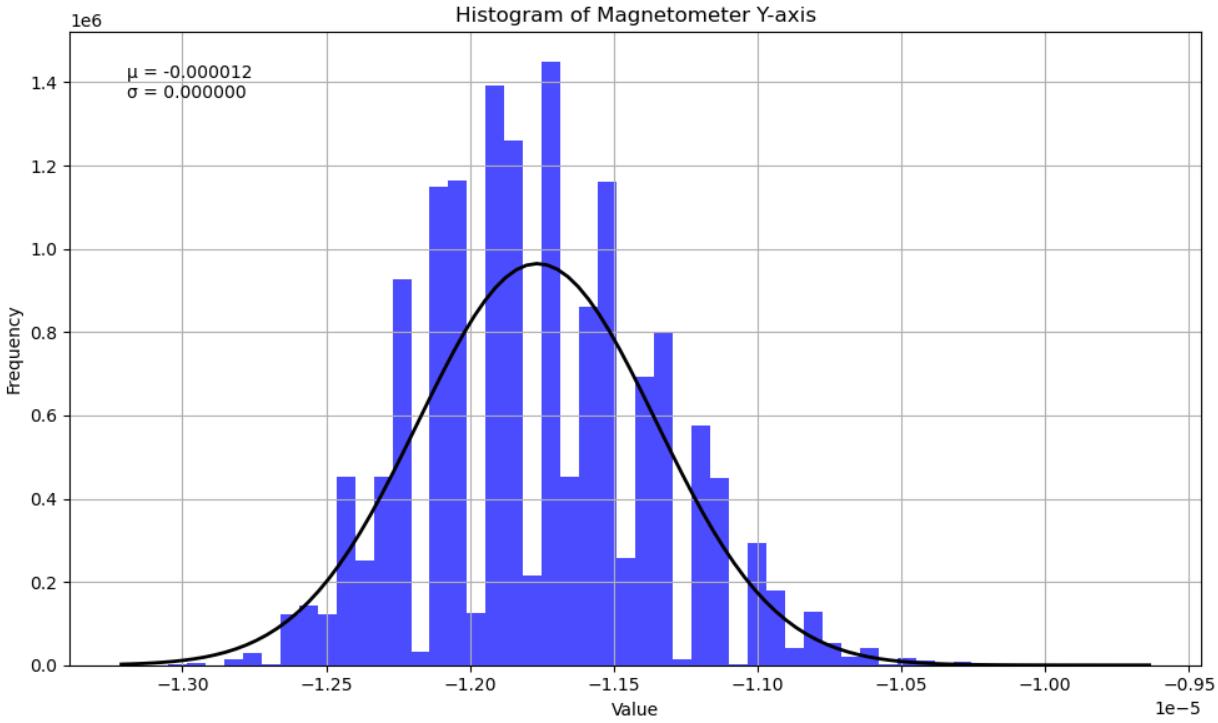

Figure 11: Histogram of magnetometer y-axis for 15-minute dataset.

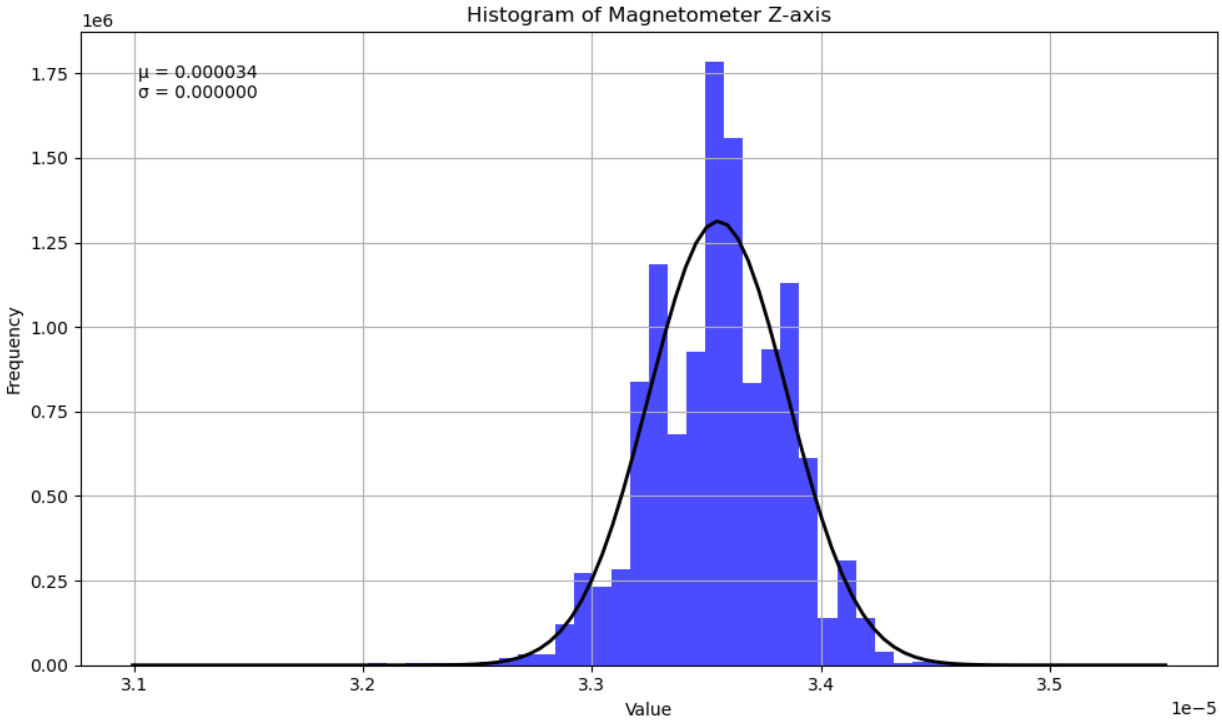

Figure 12: Histogram of magnetometer z-axis for 15-minute dataset.

3 5-Hour Data Analysis

The 5-hour stationary dataset offers comprehensive insights into the long-term behavior of the IMU sensors: accelerometer, gyroscope, and magnetometer. The primary focus of this analysis is on the Allan Variance, which provides a detailed breakdown of sensor noise and stability characteristics over varying time intervals. The results for each sensor axis are presented below.

3.1 Allan Variance Results

The Allan Deviation plots were generated for the accelerometer, gyroscope, and magnetometer axes. The key metrics from these plots include Angle Random Walk (ARW), Bias Instability, and Rate Random Walk (RRW), all of which provide crucial insights into the sensors' performance over time. Below are the calculated values for each sensor axis:

3.1.1 Accelerometer

The accelerometer data collected over the 5-hour stationary period was analyzed to determine its noise characteristics using Allan Variance. The key metrics extracted include Angle Random Walk (ARW), Bias Instability, and Rate Random Walk (RRW), which give us a detailed view of the sensor's performance over time.

- **X-axis:**
  - Angle Random Walk: $6.75 \times 10^{-1}\,\mathrm{m/s^2}/\sqrt{\mathrm{Hz}}$
  - Bias Instability: $6.27 \times 10^{-4}\,\mathrm{m/s^2}$
  - Rate Random Walk: $2.22 \times 10^{-4}\,\mathrm{m/s^2}/\sqrt{\mathrm{s}}$
- **Y-axis:**
  - Angle Random Walk: $1.34\,\mathrm{m/s^2}/\sqrt{\mathrm{Hz}}$
  - Bias Instability: $9.05 \times 10^{-4}\,\mathrm{m/s^2}$
  - Rate Random Walk: $2.47 \times 10^{-4}\,\mathrm{m/s^2}/\sqrt{\mathrm{s}}$
- **Z-axis:**
  - Angle Random Walk: $1.97\,\mathrm{m/s^2}/\sqrt{\mathrm{Hz}}$
  - Bias Instability: $1.34 \times 10^{-3}\,\mathrm{m/s^2}$
  - Rate Random Walk: $2.23 \times 10^{-4}\,\mathrm{m/s^2}/\sqrt{\mathrm{s}}$

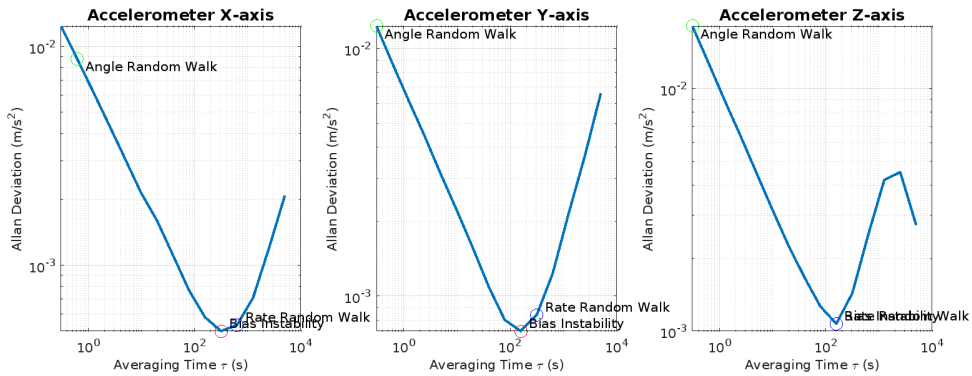

Figure 13: Allan Deviation of Accelerometer Data (5-hour stationary dataset).

Interpretation of Results

The Allan Variance results reveal the following about the accelerometer's performance:

- The **X-axis** exhibits a moderate Angle Random Walk of $6.75 \times 10^{-1}\,\mathrm{m/s^2}/\sqrt{\mathrm{Hz}}$ with relatively low Bias Instability, which indicates that the noise level is stable over time.
- The **Y-axis** has a significantly higher Angle Random Walk ($1.34\,\mathrm{m/s^2}/\sqrt{\mathrm{Hz}}$), suggesting greater noise along this axis. This could be attributed to external factors or sensor orientation during the data collection period.
- The **Z-axis** displays the highest Bias Instability value ($1.34 \times 10^{-3}\,\mathrm{m/s^2}$), indicating that this axis might experience more drift over time compared to the X and Y axes. This could impact long-term measurements if the sensor is not calibrated regularly.

3.1.2 Gyroscope

The gyroscope data collected over the 5-hour stationary period was analyzed for its noise characteristics using Allan Variance. The extracted metrics include Angle Random Walk (ARW), Bias Instability, and Rate Random Walk (RRW), which provide insights into the stability and accuracy of the sensor's rotational measurements over time.

- **X-axis:**
  - Angle Random Walk: $1.73 \times 10^{-2}\,\mathrm{rad/s}/\sqrt{\mathrm{Hz}}$
  - Bias Instability: $1.90 \times 10^{-5}\,\mathrm{rad/s}$
  - Rate Random Walk: $7.87 \times 10^{-6}\,\mathrm{rad/s}/\sqrt{\mathrm{s}}$
- **Y-axis:**
  - Angle Random Walk: $4.48 \times 10^{-3}\,\mathrm{rad/s}/\sqrt{\mathrm{Hz}}$
  - Bias Instability: $1.22 \times 10^{-5}\,\mathrm{rad/s}$

- Rate Random Walk: $8.06 \times 10^{-6}\,\text{rad/s}/\sqrt{\text{s}}$

- **Z-axis:**
  - Angle Random Walk: $9.11 \times 10^{-3}\,\text{rad/s}/\sqrt{\text{Hz}}$
  - Bias Instability: $1.32 \times 10^{-5}\,\text{rad/s}$
  - Rate Random Walk: $8.79 \times 10^{-6}\,\text{rad/s}/\sqrt{\text{s}}$

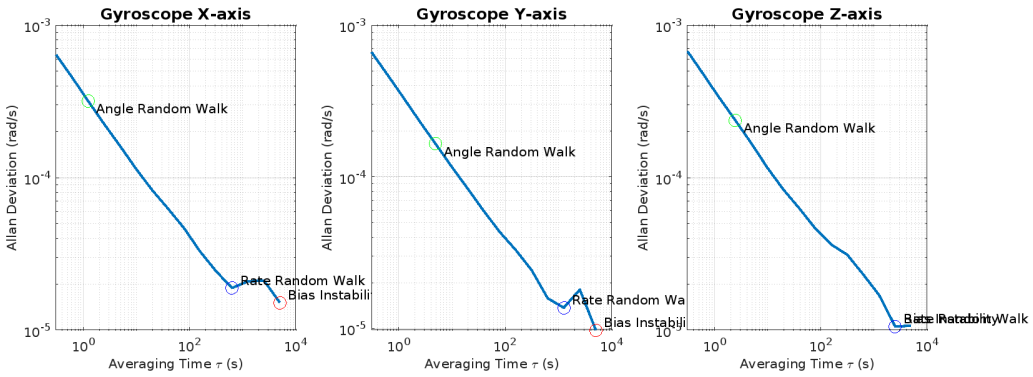

Figure 14: Allan Deviation of Gyroscope Data (5-hour stationary dataset).

Interpretation of Results

The Allan Variance results for the gyroscope indicate the following:

- The **X-axis** has a moderate Angle Random Walk of $1.73 \times 10^{-2}\,\text{rad/s}/\sqrt{\text{Hz}}$ and relatively low Bias Instability, making it stable over time, which is critical for accurate orientation tracking.

- The **Y-axis** shows the lowest Angle Random Walk ($4.48 \times 10^{-3}\,\text{rad/s}/\sqrt{\text{Hz}}$), indicating that it has less noise than the other axes. However, it still experiences some drift, as seen in the Bias Instability value of $1.22 \times 10^{-5}\,\text{rad/s}$.

- The **Z-axis** demonstrates a similar performance to the Y-axis, with a slightly higher Angle Random Walk ($9.11 \times 10^{-3}\,\text{rad/s}/\sqrt{\text{Hz}}$) but slightly lower Bias Instability ($1.32 \times 10^{-5}\,\text{rad/s}$). This suggests that while there may be noise, the Z-axis can be relied on for relatively stable measurements.

The gyroscope's Allan Deviation results highlight the sensor's overall stability in terms of rotational measurements over time, but the presence of Bias Instability across all axes indicates that regular calibration might be needed to ensure accuracy in long-term applications.

3.1.3 Magnetometer

The magnetometer data, captured over the stationary 5-hour period, was analyzed for noise characteristics using Allan Variance. The metrics obtained from the analysis include Angle Random Walk (ARW), Bias Instability, and Rate Random Walk (RRW), which offer insights into the stability of the sensor's magnetic field measurements over time.

- **X-axis:**
  - Angle Random Walk: $6.68 \times 10^{-6}\,\text{Tesla}/\sqrt{\text{Hz}}$
  - Bias Instability: $1.98 \times 10^{-8}\,\text{Tesla}$
  - Rate Random Walk: $3.76 \times 10^{-9}\,\text{Tesla}/\sqrt{\text{s}}$
- **Y-axis:**
  - Angle Random Walk: $7.88 \times 10^{-6}\,\text{Tesla}/\sqrt{\text{Hz}}$
  - Bias Instability: $4.49 \times 10^{-8}\,\text{Tesla}$
  - Rate Random Walk: $5.03 \times 10^{-8}\,\text{Tesla}/\sqrt{\text{s}}$
- **Z-axis:**
  - Angle Random Walk: $7.88 \times 10^{-6}\,\text{Tesla}/\sqrt{\text{Hz}}$
  - Bias Instability: $3.43 \times 10^{-8}\,\text{Tesla}$
  - Rate Random Walk: $1.39 \times 10^{-8}\,\text{Tesla}/\sqrt{\text{s}}$

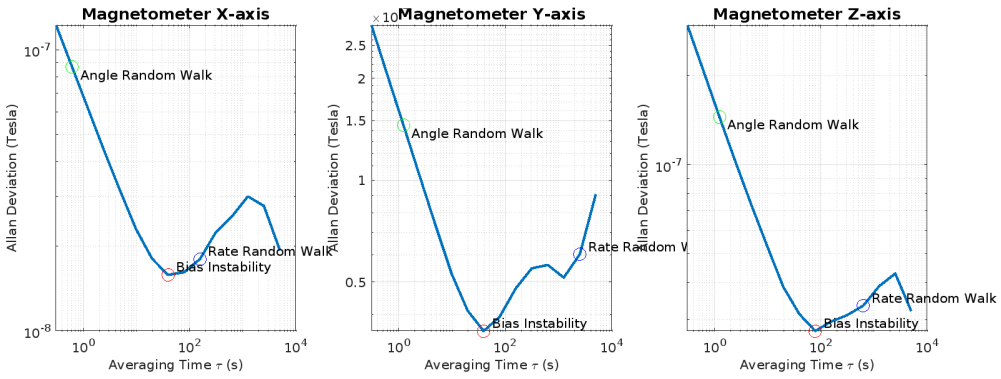

Figure 15: Allan Deviation of Magnetometer Data (5-hour stationary dataset).

Interpretation of Results

The Allan Variance results for the magnetometer show the following:

- The **X-axis** has an Angle Random Walk of $6.68 \times 10^{-6}\,\text{Tesla}/\sqrt{\text{Hz}}$, indicating relatively low short-term noise. Its Bias Instability ($1.98 \times 10^{-8}\,\text{Tesla}$) is small, suggesting minimal drift in the magnetic field measurement over time.

- The **Y-axis** has a slightly higher Angle Random Walk of $7.88 \times 10^{-6}\,\text{Tesla}/\sqrt{\text{Hz}}$, with a Bias Instability of $4.49 \times 10^{-8}\,\text{Tesla}$. This indicates more significant noise compared to the X-axis, but the sensor is still stable over time.

- The **Z-axis** shows similar performance to the Y-axis, with an Angle Random Walk of $7.88 \times 10^{-6}\,\text{Tesla}/\sqrt{\text{Hz}}$ and a Bias Instability of $3.43 \times 10^{-8}\,\text{Tesla}$. The Rate Random Walk is lowest here, suggesting consistent performance with minimal rate variation.

The magnetometer's Allan Deviation results highlight the stability of the sensor in capturing magnetic field data. The small values of Bias Instability across all axes suggest that the sensor is well-suited for long-term stationary applications, such as geomagnetic field mapping or compass-based orientation in navigation systems. However, the presence of short-term noise, as indicated by the Angle Random Walk, suggests that the magnetometer may need filtering in dynamic environments where rapid changes in orientation occur.

4 Conclusion

This report presents a detailed analysis of sensor data obtained from a stationary setup over two different periods: 15 minutes and 5 hours. The sensors evaluated include the accelerometer, gyroscope, and magnetometer, each of which was subjected to time-series, histogram, and Allan Variance analysis to characterize the noise performance and stability over time.

For the **15-minute dataset**, the time-series and histogram analysis provided insights into the distribution of noise across each axis of the accelerometer, gyroscope, and magnetometer. The data exhibited consistent behavior, with noise centered around expected values for stationary conditions. The histograms confirmed that the noise follows a near-Gaussian distribution, a hallmark of random noise with a predictable standard deviation.

For the **5-hour dataset**, Allan Variance analysis revealed critical insights into the long-term stability of the sensors. The **accelerometer** showed minimal Bias Instability and Rate Random Walk, particularly in the Z-axis, indicating robust stability in long-term applications such as navigation or motion sensing. The **gyroscope** demonstrated similarly favorable results, with low Angle Random Walk and Bias Instability across all axes, reinforcing its suitability for inertial navigation applications where long-term stability is crucial. Lastly, the **magnetometer** exhibited very low Bias Instability, making it ideal for geomagnetic field mapping or compass-based orientation over extended periods, although short-term noise remains present, as indicated by the Angle Random Walk.

Overall, the data supports the conclusion that the sensors analyzed are well-suited for both short-term and long-term stationary applications. While random noise is present in short time frames, long-term stability metrics, particularly Bias Instability and Rate Random Walk, remain low across all sensors. These characteristics are essential for applications in mobile robotics, inertial navigation, and geomagnetic field monitoring, where both short-term accuracy and long-term stability are critical. Filtering techniques may be required to mitigate the effects of short-term noise, especially in dynamic environments.The report demonstrates that, through thorough time-series and Allan Variance analysis, a comprehen-

sive understanding of sensor performance can be achieved, guiding appropriate filtering and calibration techniques for various application environments.